Original Research Article

Structural Analysis of the Bagoué furrow (South Boundiali): fracturing, kinematics and chronology

ABSTRACT

Structural mapping from spatial imagery is an important technique in controlling lineament fracture networks. The purpose of this work is to make a structural analysis of the Bagoué furrow, using spatial imagery and field data. The methodological approach adopted in the work consists in the pre-processing and digital processing of images, and the extraction of lineaments by means of automatic and manual extraction techniques. Five major lineament directions are identified: the N-S, NNE-SSW, NE-SW, E-W and NW-SE directions. The field data is used to define their kinematics and chronology. This data reveal that the lineaments corresponding to the N-S trending fractures are intersected by the NE-SW trending fractures, which in turn are cut by the NNE-SSW trending fractures. The latter are intersected by the lineaments corresponding to the SE-NW trending fractures. The SE-NW trending fractures are intersected by the E-W trending fractures. Ultimately, the N-S trending fractures are considered the oldest, followed by the NE-SW, NNE-SSW, SE-NW and E-W trending fractures.

Keywords: Lineament structures, Landsat 8, Radar, Bagoué, Ivory Coast, West Africa

1. INTRODUCTION

Structural analysis in geological sciences is of paramount importance in the exploration of mineral resources [1]. However, in tropical regions such as Côte d'Ivoire, it is not an easy task to identify lineament structures because of the thick lateritic cover over the geological substratum. Therefore, the use of remote sensing data processing techniques in structural analysis based on lineament mapping has become an important approach in geological studies. Lineaments are thus regarded as important structural and tectonic indicators to determine regional tectonic trends and fracture zones in rocks [2]. These structural features can then constitute preferential flow paths for hydrothermal fluids and groundwater [3]-[5]. By offering a synoptic view, remote sensing allows for the study of vast geographical areas and it is also a powerful tool in analyzing fracturing [6].

The main objective of this work is to carry out a structural analysis of the Bagoué furrow using spatial images. This will specifically include the mapping of all the fracture networks of the Bagoué furrow (South Boundiali) by extracting the lineament networks from satellite images while validating those using structural field data, and then the establishment of their kinematics and chronology relative to the regional scale.

2. STUDY AREA AND GEOLOGICAL CONTEXT

The Bagoué Trench is located in the northwest of Côte d'Ivoire (West Africa) and more precisely in the Bagoué region. It is therefore located between longitudes 6°00 and 7°00 W and latitudes 8°00 and 10°00 N. In this area, the water regime is known as the transitional tropical regime, with the Bagoué River as its main watercourse.

The Bagoué Trench is an entity of the Boundiali-Bagoé Birimian unit, whose geology is an integral part of the Baoulé-Mossi domain of the West African Craton. The geological formations are of Paleoproterozoic era and are characterized by a succession of bands of schistose rocks, migmatitic rocks and plutonic rocks. Thus, one can observe from west to east of the complex of undifferentiated granites with some areas of biotite granites, granites with marked migmatitic facies and porphyroid

granite. In a few places, these granites are associated to basic rocks [8]. Next to these granites, there is a zone of undifferentiated schists and sericite schists. The geological formations are also characterized by the presence of a band of biotite granite, and granitoids and calc-alkaline granite with amphibole in the southeast (Fig.1).

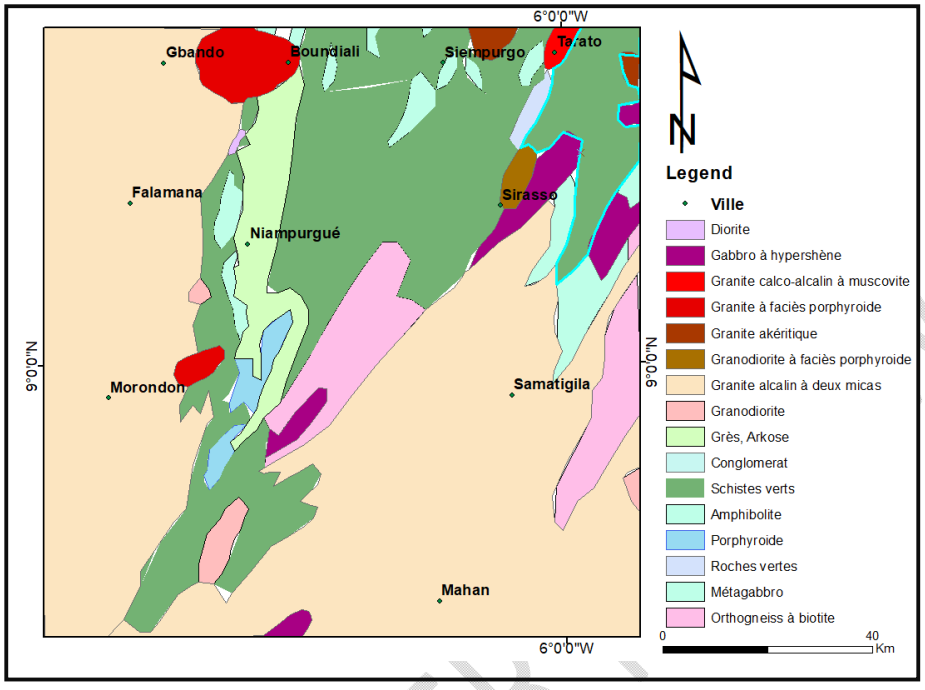

Fig. 1. Geological map of the Bagoué furrow as modified by [9]

3. MATERIAL AND METHODS

3.1 MATERIAL

In this study, the mapping databases used include the topographical and geological maps of the Bagoué region at 1:200,000 scale and then the field data. The data used for the extraction of the linear network are from orthorectified Landsat 8 OLI optical images composed of four scenes (197-053 of 29/12/2019, 197-054 of 29/12/2019, 198-053 of 04/12/2019 and 198-054 of 04/12/2019) covering the study area, and also from radar images (SAT and ERS radar).
The geographic information system software used in this study includes: Envi 4.7, used to carry out various tasks of image preprocessing and processing; PCI's Geomatica for the automatic extraction of the lineament network through its LINE module; Arcgis 10.4, used to extract the statistical parameters of the lineaments and to dress maps; Adobe Illustrator to digitize the manually extracted lineaments and then Georient and RockWorks 17 to generate rose diagrams.

3.2. METHODOLOGY

Two methods for extracting lineaments from spatial images were used in this work: automatic extraction by the use of the LINE module of Geomatica and visual extraction by which lineaments are detected by visual interpretation. The preprocessing and processing techniques have allowed for the automatic and manual extraction of lineaments from OLI images and radar images.
The methodological approach adopted for the mapping of geological lineament structures is summarized in the following diagram (Fig. 2).

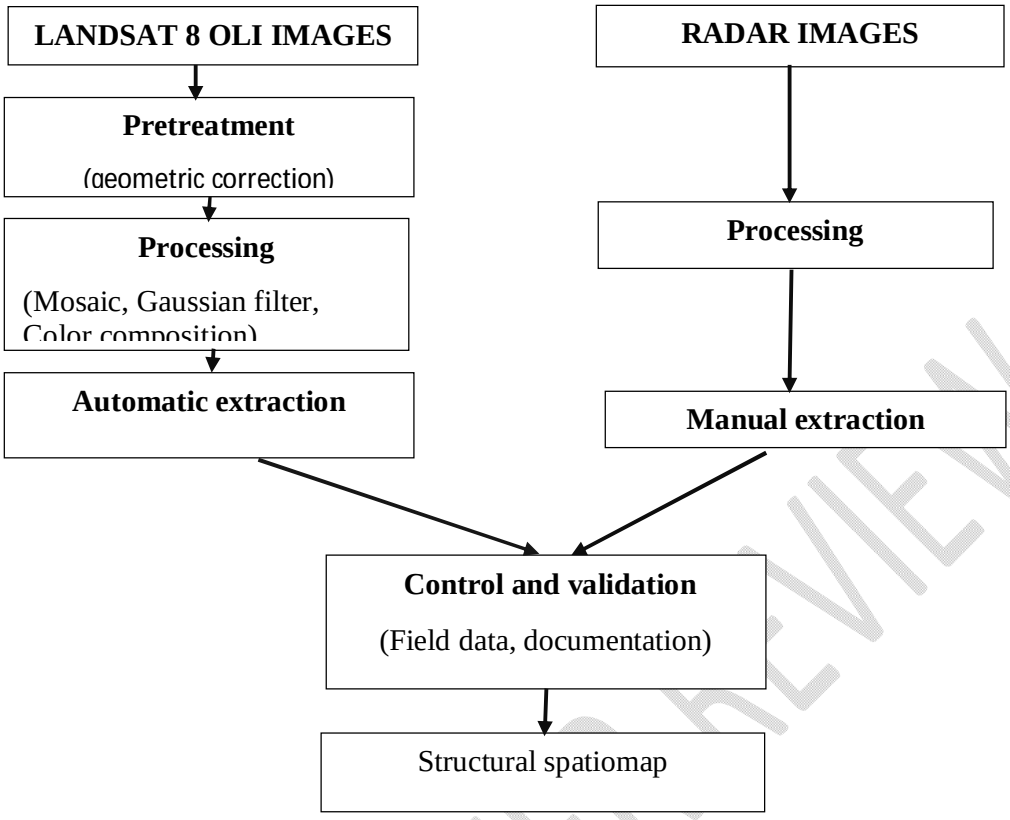

Fig. 2. Landsat 8 image and radar images processing methodology

4. RESULTS AND DISCUSSION

The mapping in our study area initially consisted in the digital processing of Landsat 8 optical satellite images and radar images, of which some results are shown in Fig.3.

4.1. EXTRACTION OF LINEAMENTS

In this study, the extraction of lineaments is based on Landsat 8 OLI satellite images along with radar images (SAT and ERS radar). This is carried out both by automatic and manual extraction techniques. The results obtained from the automatic extraction technique have allowed for the identification of 12930 lineaments (Fig. 4). This fig. 4 shows that the map of the automatically detected lineament is very loaded. Therefore, the different patterns of geological lineaments are not revealed. However, the N-S and NE lineament trends are well highlighted.

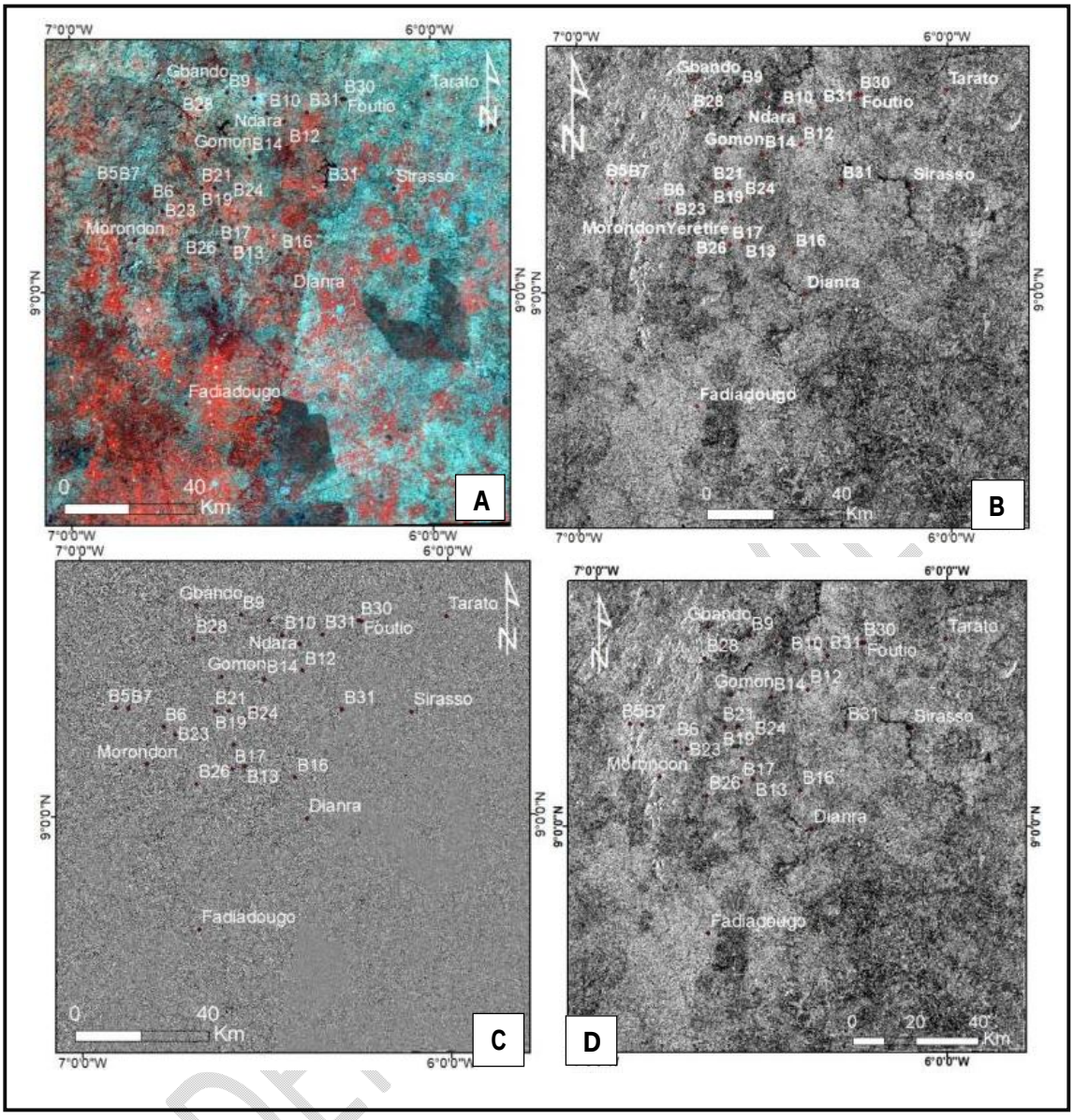

Figure 3. Landsat 8 OLI image and radar image processing. (A): Color-coded (567) OLI image; (B): Image filtered by Gaussian high pass filter applied on band 8 of OLI image; (C): Radar SAT image; (D): Radar ERS image (negative print)

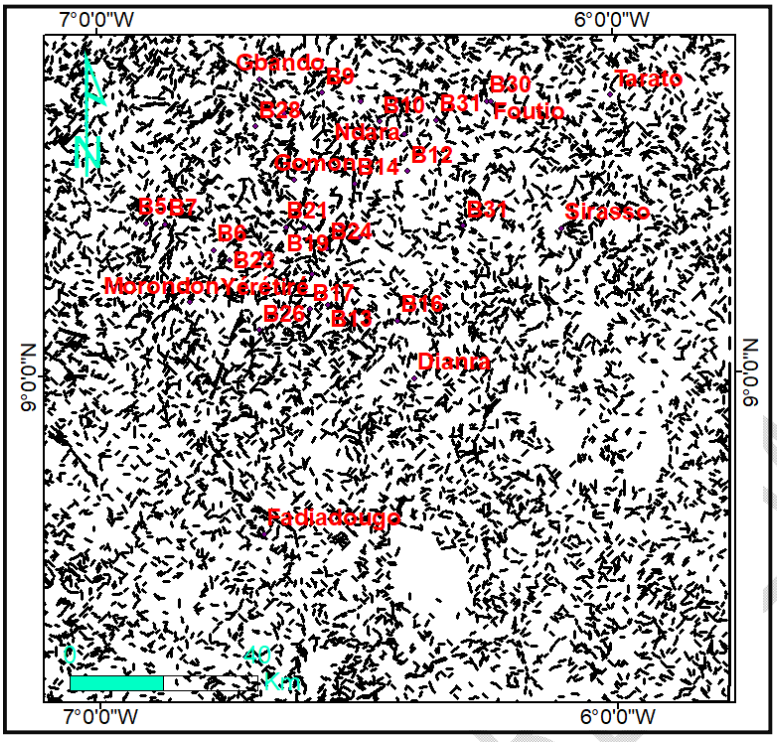

Fig.4. Map of the automatically detected lineaments

The lineament texture analysis of the maps generated from manual extraction (Figures 5 and 6) shows the following geometric shapes:

- arc-shaped lineaments, ovoid to radial representing periplutonic to plutonic areas [10], [11],
- large rectilinear lineaments that most often correspond to large regional fractures, and
- small straight lineaments.

Of the two lineament maps deriving from manual extraction, that of SAT radar image reveals more lineament structures with arc-like shape than that of ERS radar images. The latter also has fewer lineament structures compared to the former.

The manual extraction technique is used to extract lineaments from SAT and ERS radar imagery. This technique was useful in detecting long geological lineaments in the NE and NW directions and medium lineaments in the E-W and NS directions of the study area in both radar images (Fig. 5 and 6).

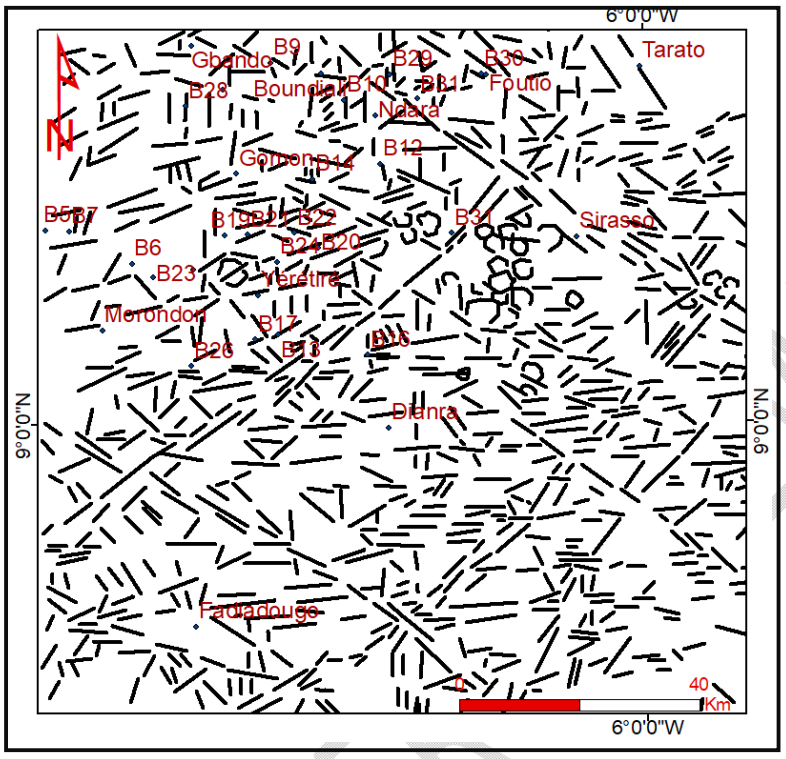

Fig. 5. Map of the lineaments extracted manually from radar SAT image

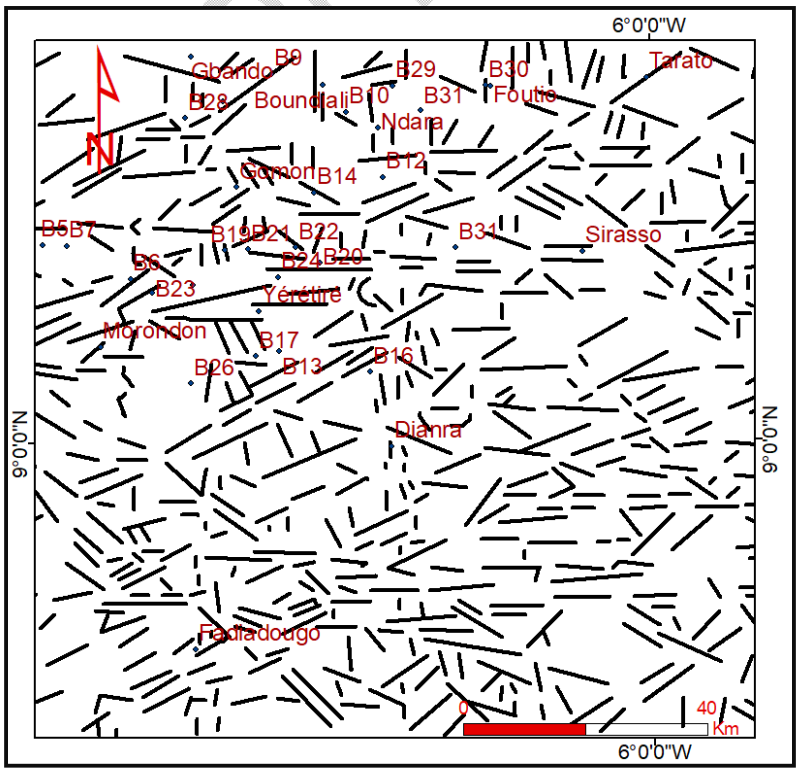

Fig. 6. Map of the lineaments extracted manually from radar ERS image

4.2 DIRECTIONAL STATISTICAL ANALYSIS OF THE LINEAMENT MAPS

The directional statistical analysis of the synthetic maps of the structural lineaments extracted from our study area (Fig. 7), shows a dispersion of structural lineaments in all directions (N0° to N180°). Among these directions, five major groups of directions stand out in the diagrams that discriminate lineament orientations of the maps in fig. 5 and 6: 1) N-S direction lineaments (N00° to N10°), 2) NNE-SSW direction lineaments (N30° to N40°), 3) NE-SW direction lineaments (N40° to N50°), 4) E-W direction lineaments (N90° to N100°), and 5) SE-NW direction lineaments (N130° to N140°); and six minor direction groups: N10° to N30°, N50° to N70°, N70° to N90°, N110° to N120°, N120° to N130° and N140° to N170°.

The directional statistical analysis of the map of the automatically extracted lineaments (Fig. 7A) allows us to highlight four classes of preferential directions: 1) the class of N-S direction (N00° to N10°), 2) the class of NE-SW direction (N40° to N50°), 3) the class of E-W direction (N90° to N100°) and 4) the class of NW-SE direction (N30° to N40°).

The overall directional analysis of the three maps shows the following:

- the lineament maps in Fig. 4 and 6 show a significant number of lineaments with N-S and E-W directions compared to the lineament map in Fig. 5,
- the maps in fig. 5 and 6 show more discriminable and concordant lineament directions compared to those of the map in fig. 4,
- the NNE-SSW and NE-SW lineaments in Fig. 5 are more numerous than those of the lineaments in Fig. 6. Furthermore, they are more numerous in the E-W direction in Fig.6 than in fig. 5,
- the map in Figure 4 is highly saturated.

As a result of the directional statistical analysis of the lineament maps, one of the maps of the lineament extracted manually is retained and used for the control and validation of the lineaments. This is the lineament map extracted from radar SAT image (Fig. 5) which shows almost all the lineament structures that can be found in the field.

4.3 CONTROL AND VALIDATION OF LINEAMENTS

The control and validation phase of the geological lineaments of our study area consisted in comparing the preferential directions of the lineaments extracted manually from the SAT radar image and in confronting them with the results of field works. This control phase is essential in assessing the relevance of the chosen extraction method and the results obtained.

Using field data in control phase is an adequate means to validate structural lineaments. The study site which is located in a basement environment with a subhumid tropical climate, is largely covered with lateritic crust and laterite, which explains the scarcity of outcrops in this area. Few data have been collected in the field regarding this rarity of outcrops. The geotraverse carried out in the field made it possible to observe metasediments in Tarato in which schistosity networks develop with fractures trending N160-60W, N60-50NW (Fig. 9 C). The N160° fractures intersect those of N60° following a sinistral movement. In Foutio, not far from Tarato, they are schistosity networks with fracture N60° intersected by N170° schistosity and N160 quartz veins dipping northeast which intersect the N90° quartz veins dipping vertically (Fig. 10A). In the field, several measurements were taken which led to the realization of the rose diagrams that discriminate the directions of fractures. The rose diagram (figure 8) shows seven families of fractures observed in the study area: 1) fractures trending N0° to N20°; 2) fractures trending N30° to N40°; 3) fractures trending N50° to N60°; 4) fractures trending N70° to N100°; 5) fractures trending N120° to N130°; 6) fractures trending N140° to N150 and 7) fractures trending N160° to N170°. Among these families, there are four preferential directions: fractures trending NNE-SSW (N10° to N20°), fractures trending NE to SW (N50° to N60°), fractures trending EW (N80° to N90 °) and fractures trending SE-NW (N120° to N130°).

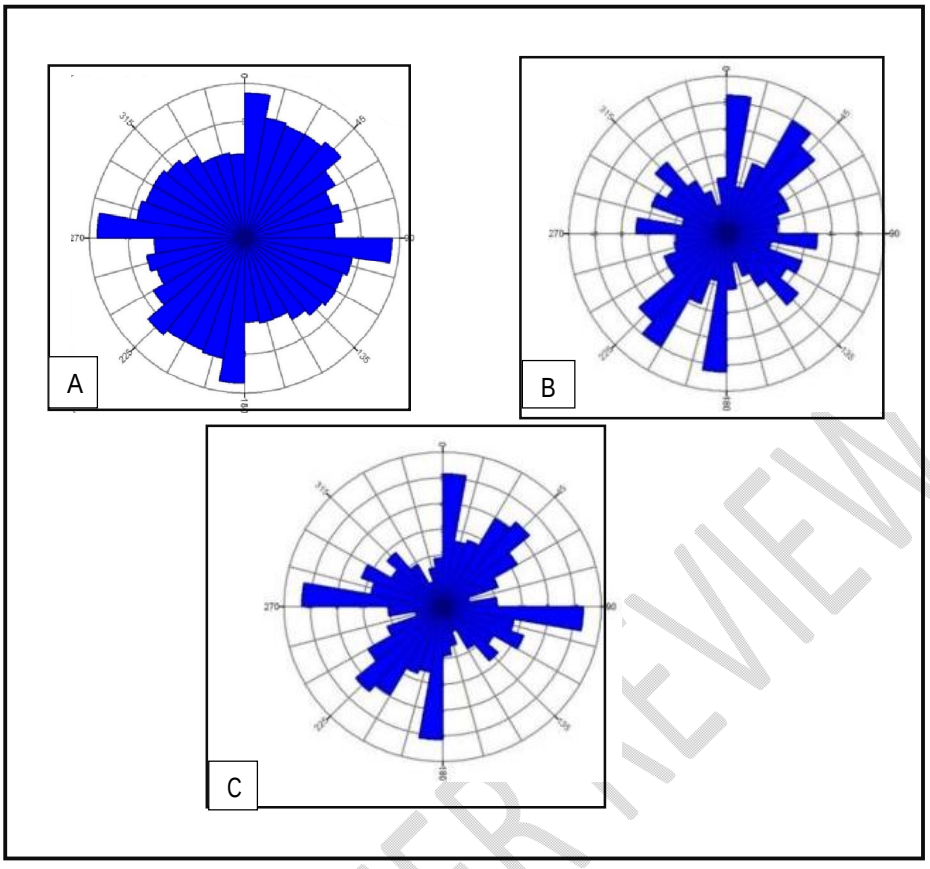

Figure 7. Directional statistical analysis. (A): Rose diagram of the lineaments extracted automatically; (B): Rose diagram of the lineaments extracted manually from radar Sat image; (C): Rose diagram of the lineaments extracted manually from radar ERS image

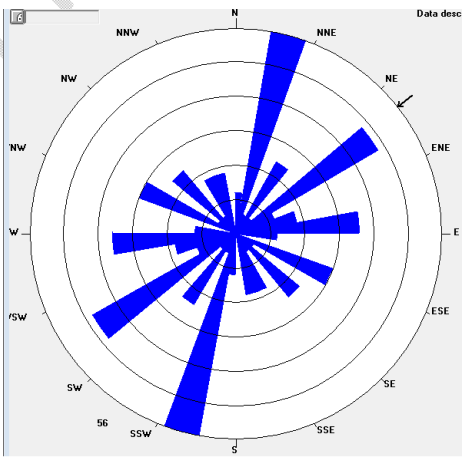

Fig. 8. Drectional rose of the fractures in the study area

The spatial analysis in the field reveals that the NE direction fractures are intersected by the NNE direction fractures following a sinistral shear. The latter are in turn intersected by fractures trending SE in a sinistral shear context. SE trending fractures are intersected by E-W trending fractures by dextral shear. N-S trending fractures are intersected by NE trending fractures following a sinistral shear.
From a chronological point of view, N-S fractures are older, successively followed by NE-SW, NNE-SSW, SE-NW fractures and E-W fractures which are considered as the youngest according to the intersection principle.

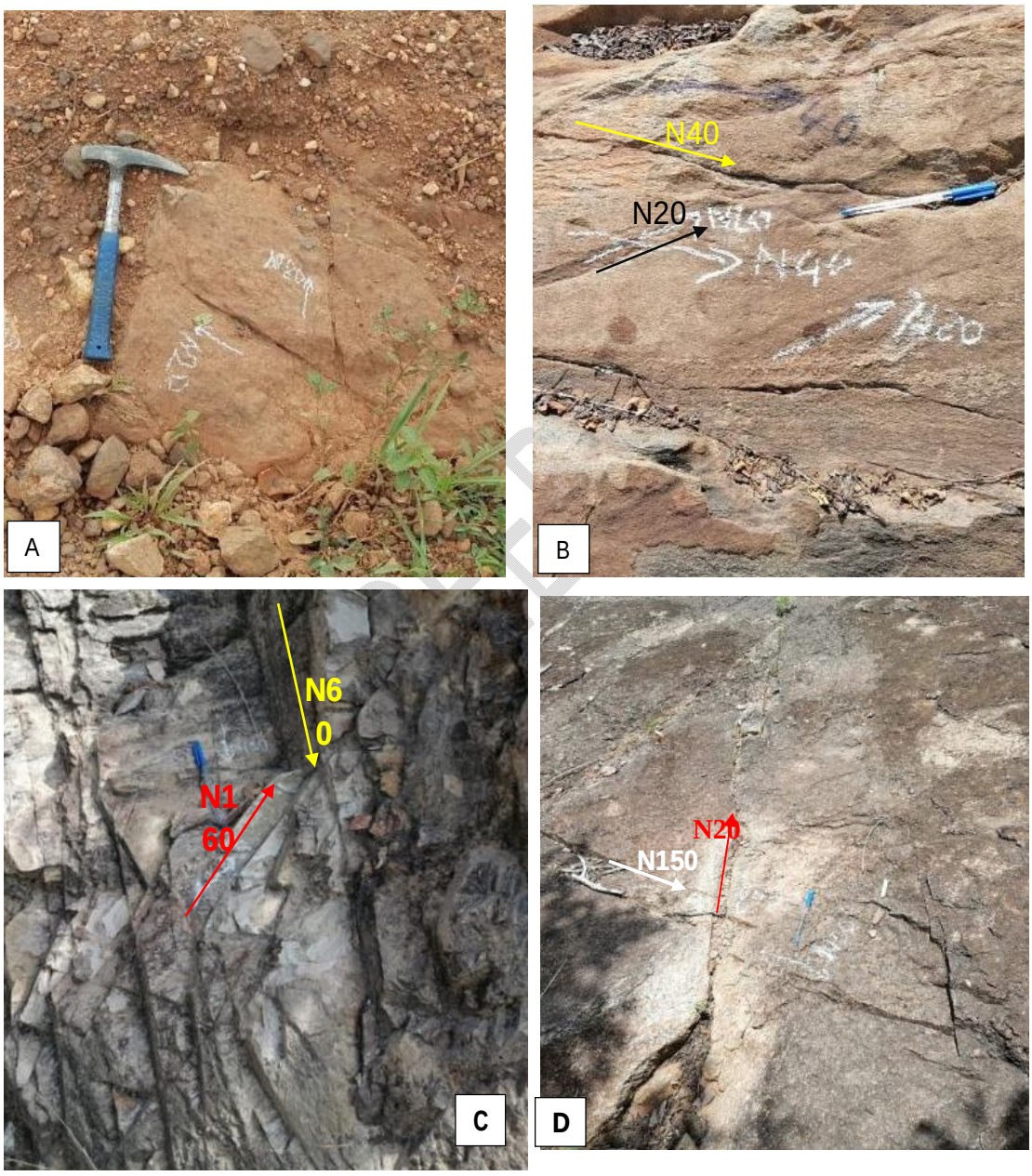

Fig.9. (A): Outcrop of fractured metasediments with intersecting fractures; (B): Outcrop of diorite affected by the N20° fractures intersecting the N40° fractures in dextral shear; (C): Folded metasediments presenting fractured networks, the N160° networks intersect the N60° networks; (D): Outcrop of fractured gneiss with N150° fractures intersecting the N20° fractures.

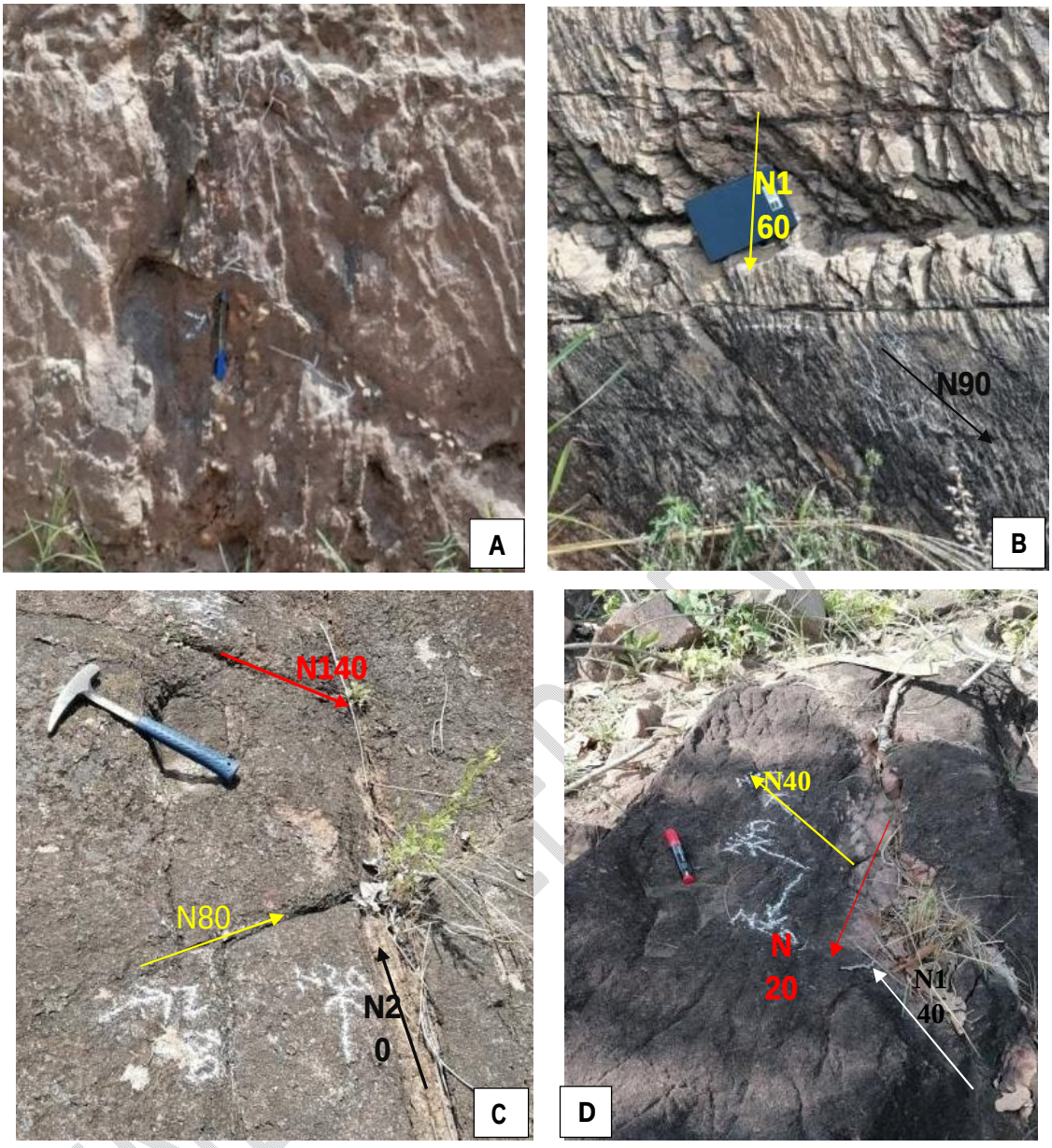

Figure 10. Lithological and structural data about some of the outcrops in the study area. (A) : Outcrop of metasediments in which the N160 quartz veins intersect the N90° veins (B) : Fractured metasediment with N170° and N60° fractures intersecting; (C) : Fractured biotite granite outcrop, the N20° fractures are intersected by the N140° fractures and both fracture networks are intersected by N80° fractures; (D): Fractured biotite granite outcrop with directions: N20° intersected by N140°, N40° intersected by N20°.

The validation of the lineaments extracted by analogical analysis consisted in comparing the statistical data of the lineament network with those of the field and in establishing genetic links between them. In order to assess the contribution of the spatial imagery data, the lineaments extracted from them were compared to the structural data collected in the field. Two objectives are considered for this comparison: the reliability of the interpretation of the lineament analysis and the spatial precision of the data collected in the field.

The field data, by analogy with the orientations of lineaments, allowed to draw up the following synthesis: the direction families deriving from the lineament map are similar to those shown by the field data on the directional rose diagram (fig.10). Nevertheless, some lineaments from satellite

images are not remarkable with the structural elements of the terrain. These lineaments belong to the following directional classes: N20° to N30°, N40° to N50°, N60° to N70°, N100° to N110°, N120° to N130°, N140° to N150° and from N170° to N180°. Other families of lineaments, on the other hand, are superimposable on those of the structural elements of the terrain; these are particularly the families of directions N00° to N20°, N30° to N40°, N50° to N60°, N70° to N100°, N110° to N120°, N130° to N140° and from N150° to N170 °.

Following the validation of the lineaments by structural field data, the lineament map resulting from the SAT radar image represents the final map of the fractures affecting the Bagoué furrow.

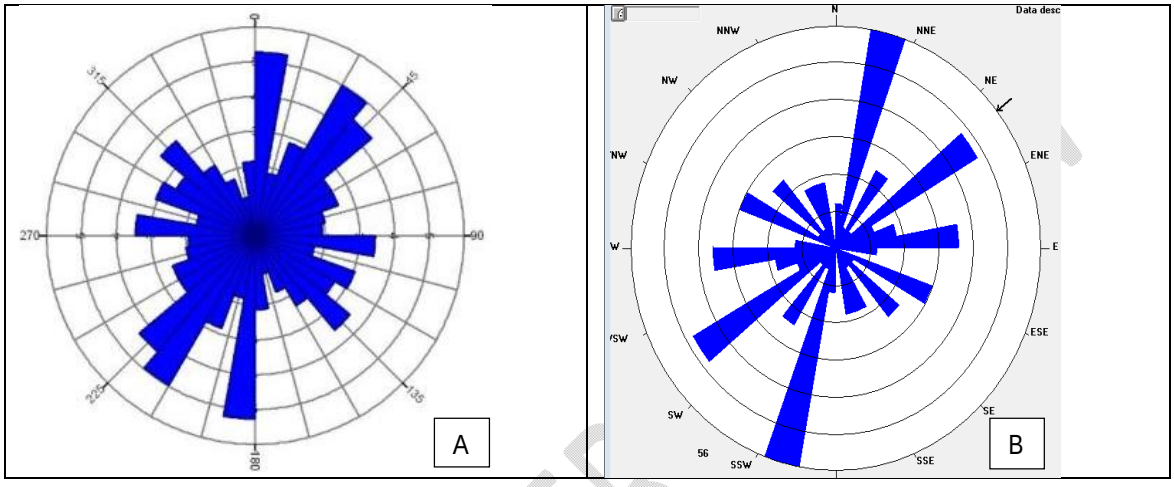

Figure 11. **Comparison of the directional rose diagrams. (A): the lineaments extracted from SAT radar image; (B): field data.**

4.4 DISCUSSION

Satellite image processing for the purpose of structural mapping made it possible to detect the lineament structural elements of the Bagoué furrow. To ensure the reliability of this mapping technique, the structural field data was checked by reference to the lineaments extracted from spatial imagery through the comparison of the directional rose diagrams. The rose diagrams analysis shows that some families of lineaments extracted from satellite images are perfectly superimposable on the structural elements of the field, others are slightly offset and they do not appear on the rose diagram of the field data and other families are in the same extension as the latter but are not superimposable on them. The discrepancy between satellite lineaments and the structural elements of the field is explained by the geocoding and resampling effect which cause inaccuracy in the processed images [12], [13], [14]. The absence of certain families of lineaments (N20° to N30°, N40° to N50°, N60° to N70°, N100° to N110°, N120° to N130° and N140° to N150°) on the rose diagram of the field data can be attributable to the scarcity of outcrops which did not allow for the observation of these families of structures during the geotraverse in the field. The N20° to N30° lineament classes have been highlighted on the kolia granite outcrops by [15]. Lineament classes N120° to N130° were observed by this same author on the Boundiali arkoses. These lineaments families which were not noticed in the field during our study were observed on the Bagoué furrow by [9] and [15]. From the above analyses, the similarity between the directional rose diagrams of the lineaments with the directional rose diagrams of the field data and the previous studies carried out on the Bagoué furrow do confirm that the lineaments extracted from satellite images correspond to geological fractures. The lineament map (fig 5) resulting from manual extraction using SAT radar imagery is then the structural map of the Bagoué furrow. On this map, the arc-shaped lineaments, ovoid to radial which can be observed in the

northeast correspond to the relics of the periplutonic and plutonic zones whose laminations constitute real gold traps [10]. The directional analysis of the lineaments highlights five preferential directions: NS (N00° to N10°), NNE-SSW (N30° to N40°), NE-SW (N40° to N50°), EW (N90° to N100 °) and NE-SW (N130° to N140°). The NNE-SSW trending Lineaments might correspond to the direction of orientation of the general schistosity indicated by the mineral schistosity of direction N20° which can be observed on the granitoid outcrops located in the South-west of the study area and the schistosity of N20° to N30° trending fractures observed in volcano-sedimentary and sedimentary rocks. NE-SW trending lineaments define the direction of the high to medium density lineaments on the ground. They correspond to the Yérétiélé faults described in the Bagoué furrow by [21].

5. CONCLUSION

For the structural analysis of the Bagoué furrow using space imagery, we had to use Landsat 8 OLI satellite images together with radar images. The chosen methodological approach to achieve the objective of this study is based on image pre-processing and processing operations in order to enhance the images and extract lineament structures. The automatic and manual lineament extraction techniques led us to retain the lineament map manually extracted from the SAT radar image because of its conformity with the geological structures of the area of interest.
The statistical analysis of the lineament network using the directional rose diagrams showed a particular directional distribution of these lineament structures. They are organized into five main directional systems: N-S, NNE-SSW, NE-SW, E-W and NW-SE. These lineament directions correspond to zones with medium to high fracture density. From a chronological point of view, the lineaments corresponding to the N-S trending fractures are intersected by the NE-SW trending fracture zones moving in a sinister direction, which in turn are intersected by the NNE-SSW direction fracture zones moving in a sinister direction. The latter are intersected by the lineaments of the SE-NW trending fracture zones moving in a sinister direction. The SE-NW fracture zones are intersected by the E-W fractures in a dextral movement. In the end, the lineaments corresponding to the N-S direction fracture zones are considered to be the oldest, followed successively by the NE-SW, NNE-SSW, SE-NW and E-W direction fracture zones, which are considered to be the youngest.
The resulting structural map obtained using spatial imagery will constitute the structural map of the Bagoué trench and will help to update the previous structural maps of the area. It will serve as a guide for mineral and water resource exploration activities.

REFERENCES

1. Marghany M, Hashim M. Lineament Mapping Using Multispectral Remote Sensing Satellite Data, Research J. of Applied Sciences. 2010; 5(2): 126-130. doi: 10.3923/rjasci.2010.126.130.
2. El-Sawy ESK, Ibrahim M, El-Bastawesy MA, El-Saud WA. Automated, manual lineaments extraction and geospatial analysis for Cairo-Suez district (Northeastern Cairo-Egypt), using remote sensing and GIS. 2016; 3(5):10.
3. Christian AG, Sekouba O, Alexis KK., Bachir M, Fernand KK. Automatic extraction of lineaments using optical and radar satellite images in the middle of the Precambrian basement (Haute Marahoué, Côte d'Ivoire. 2019; 8(01): 24-32.
4. Nouayti M, Khattach N D, Hilali M. Mapping of potential areas for groundwater storage in the upper Ziz basin (Morocco): Contribution of remote sensing and geographic information system. 2017;13.
5. Zazoun RS, Marok A, Samar L, Benadla M, Mezlah H. Fracturing and deformation bands in the El Kohol region (Central Saharan Atlas, Algeria): fractal analysis, scaling laws and network model discrete fractures. 2015 ; 71(2); 39. doi: 10.3989/egeol.42011.359.
6. Millogo C, Nakolendoussé S, Saga S. Mapping of geological accidents by satellite imagery and airborne geophysics, and statistical analysis of the fracture networks of the Birimian basement of the Lake Bam watershed (northern center of Burkina). 2018.
7. Beaudou AG, Sayol R. Soil study of the Boundiali - Korhogo region (Côte d'Ivoire): cartography and summary soil typology, Boundiali sheet, Korhogo sheet at 1/200,000. 1980; 58.
8. Eschenbrenner V, Badarello L. Pedological study of the Odienné region (Ivory Coast): map of morpho-pedological landscapes, O.R.S.T.O.M., Paris. 1978.

9. Turner P. Evolution of the early Proterozoic Boundiali-Bagoe Supracrustal Belt and associated granitic rocks, northern Côte d'Ivoire, West Africa. », PhD, University of Portsmouth, 1995.
10. Niamke K H. Remote sensing and GIS in mining prospecting strategy 1 in Côte d'Ivoire: case of the Baoulé-Est 1 gold index of the n'Zi Comoé region (central Côte d'Ivoire)", University of Cocody. 2008.
11. Gbele O. (1998) "Structure of the Ferkessédougou batholith (zuenoula sector, Ivory Coast): implications for the interpretation of the geodynamics of the Paleoproterozoic of West Africa at 2.1 Ga", Doctoral thesis from the University of Orléans.1998; 344.
12. Guillaume R. Development and evaluation of new methods for the spatial-spectral classification of hyperspectral images. Doctoral thesis from the University of Toulouse. 2012;148.
13. Sghaier MO. Extraction of linear structures from very high resolution satellite images to help in the management of major disasters. Doctoral thesis, École de technologie supérieure university of Quebec. 2017; 270.
14. Yao KA. The volcanism of the Boudali furrow, the main phenomenon of the Lower Proterozoic in this NNW region of Côte d'Ivoire. Doctoral thesis, University of Clermont-Ferrand 2. 1993; 201.
15. Gnammytchet Barthelemy Koffi. Possibilities and limits of ers radar images in geological mapping. Application in Ivory Coast". Doctoral thesis, University of Paris 6. 1998.